NY 87-22-4 (RP-409)

PERFORMANCE AND CONTROL CHARACTERISTICS OF A LARGE COOLING SYSTEM

J.E. Braun, P.E. **J.W. Mitchell, Ph.D.** *ASHRAE Member* **S.A. Klein, Ph.D.** *ASHRAE Member*

W.A. Beckman, Ph.D., P.E.

ABSTRACT

Results concerning the performance and control characteristics of the Dallas/Fort Worth (D/FW) cooling system are presented. Computer simulation models of the equipment are presented and compared with measurements for the D/FW plant. The performance associated with the use of variable-speed chiller control is compared with that of fixed speed vane control. Interactions between the control of the chiller, condensing pumps, and cooling tower fans are investigated in detail. Methodologies useful for optimal control of large cooling systems are developed.

INTRODUCTION

This paper presents results of an investigation of the performance and control characteristics of the cooling system at the Dallas/Fort Worth airport. This particular system is of general interest because of the large data acquisition system and the unique retrofits that the plant personnel have undertaken.

The data acquisition system records a wide range of conditions on magnetic tape each minute. This information is invaluable in developing and validating computer simulation models of the equipment that is used in evaluating both improved control strategies and retrofits for the plant.

Several retrofits have been implemented at the D/FW plant to reduce energy consumption. Foremost among these was the conversion of the drive for the primary centrifugal chiller. The cooling plant has three centrifugal chillers, originally rated at 8700 tons (30.6 MW) each. Each of these chillers as initially installed was driven with a steam turbine. As a result of poor turbine efficiencies at low speeds, these chillers were primarily operated at fixed compressor speeds. The capacity modulation was provided by control of inlet prerotation and outlet diffuser vanes. Through good energy management practices, the energy consumption at the D/FW has been reduced to the point where a single chiller provides the necessary cooling almost all year long. To further reduce energy consumption at part-loads, the primary chiller was retrofit with a variable-speed electric motor. At the same time, the chiller refrigerant was changed from R-22 to R-500 and the chiller capacity was derated to 5500 tons (19.3 MW). This cooling capacity in conjunction with the use of storage is sufficient most of the time to satisfy the system demand. Additional retrofits at the D/FW include conversion of distribution pumps and cooling tower fans to variable-speed motors.

J.E. Braun, Research Assistant, J.W. Mitchell, S.A. Klein and W.A. Beckman, Professors of Mechanical Engineering, University of Wisconsin-Madison.

Goals of the study reported here were to:

1. Define appropriate computer models for the equipment used in large cooling plants and compare with data from the D/FW system.

2. Document the improvements in performance associated with the use of variable-speed control for the centrifugal chiller as opposed to fixed-speed operation with vane control.

3. Study the control characteristics of the D/FW plant in order to identify good control practices and to determine the energy savings resulting from the use of optimal control.

4. Develop methodologies necessary for implementing on-line optimal control of the equipment in large cooling plants.

COMPONENT MODEL DEVELOPMENT AND VALIDATION

In this section, simple models of chilled water equipment, appropriate for system simulation, are developed and compared with measurements from the D/FW airport. Models are presented for variable-speed and fixed-speed chillers, cooling towers, and pumps.

Empirical Chiller Model

A companion paper (Braun, et al. 1987) describes a detailed mechanistic model that is useful for investigating the performance of a variable speed chiller. However, it requires too much computation to be used in system simulation studies in which seasonal performance calculations are made. Results of this detailed model indicate that the chiller power consumption is primarily a function of only two variables, the load and the temperature difference between the leaving condenser and chilled water flows. The following functional form was suggested by Johnson (1985) for estimating chiller power.

$$\frac{P_{ch}}{P_{des}} = a_0 + a_1X + a_2X^2 + a_3Y + a_4Y^2 + a_5XY \qquad (1)$$

where X is the ratio of the load to a design load, Y is the leaving water temperature difference divided by a design value, P_{ch} is the power consumption, and P_{des} is the power associated with the design conditions. The empirical coefficients of the above Equation (a_0, a_1, a_2, a_3, a_4, and a_5) are determined with linear least-squares curve-fitting applied to measured or modeled performance data.

Measurements from the D/FW facility were fit to Equation 1 with design conditions taken to be those associated with the maximum measured power consumption. Table 1 shows good agreement between the data and the model. The root-mean-square of the error of the power relative to the design power is 0.018.

Equation 1 can also be used to fit data for a chiller operated at a fixed speed with inlet vane control. Table 2 compares results of curve fits to data with the measurements. The agreement is not quite as good as for the speed control. The relative rms error is 0.042. These larger errors are most likely due to a more unstable control characteristic in fixed speed operation as discussed later.

Cooling Tower Models

The most common model of the performance of cooling towers is the Merkel method outlined in the ASHRAE Handbook-1983 Equipment Handbook. The cooling tower is divided into nodes in the direction of the air and water flows. To predict the outlet states requires an iterative solution. Each iteration involves a numerical integration of the heat transfer rate across the two flow streams through the tower.

A simpler approach that does not involve a numerical integration was developed by Whillier (1967) and is utilized in this study. A tower effectiveness is correlated in terms of the ratio of thermal capacities of the air and water streams. This effectiveness is then used directly to determine the exit states of the air and water.

An energy balance on the flow streams (neglecting the fan work input) yields the following relationship.

$$m_a(h_{a,o} - h_{a,i}) = m_{cw}C_{pw}(T_{cwr} - T_{cws}) + m_a(\omega_o - \omega_i)C_{pw}T_{cws} \quad (2)$$

where

m_a = the air flow rate
$h_{a,o}$ = enthalpy of the exiting air and water mixture
$h_{a,i}$ = enthalpy of the entering air and water mixture
m_{cw} = mass flow rate of tower water from chiller condenser
C_{pw} = specific heat of water
T_{cwr} = return temperature of chiller condenser water (supply to tower)
T_{cws} = supply temperature to chiller condenser (return from tower)
ω_o = humidity of exit air
ω_i = humidity of inlet air

Most analyses neglect the energy term associated with the water loss (last term of Equation 2). In order to account for it in an approximate manner, Whillier utilized a grouping of terms called "sigma energy," h_s. Applied to the inlet air stream, the "sigma energy" is defined as

$$h_{s,i} = h_{a,i} - \omega_i C_{pw} T_{wb} \quad (3)$$

where T_{wb} is the wet bulb temperature.

With this definition and neglecting the additional terms involving the humidity ratio, Equation 2 becomes

$$m_a(h_{s,o} - h_{s,i}) = m_{cw}C_{pw}(T_{cwr} - T_{cws}) \quad (4)$$

In Whillier's analysis, the left- and right-hand sides of the above equation are each considered to be the heat transfer rate from the water to the air stream, Q_{tower}, although this is not strictly correct. Analogous to the use of C_{min}/C_{max} in heat exchanger theory, the ratio of the minimum to maximum thermal capacities of the cooling tower streams, termed the tower capacity factor, is

$$R = \frac{\text{Min}(Q_{a,max}, Q_{w,max})}{\text{Max}(Q_{a,max}, Q_{w,max})} \quad (5)$$

where the maximum possible heat transfers to each stream are

$$Q_{a,max} = m_a(h_{s,cwr} - h_{s,i}) \quad (6)$$

$$Q_{w,max} = m_{cw}C_{pw}(T_{cwr} - T_{wb}) \quad (7)$$

and $h_{s,cwr}$ is the maximum possible "sigma energy" of the exiting air at the temperature of the entering water, T_{cwr}.

Cooling tower effectiveness is defined as the ratio of the actual to maximum possible heat transfer from the water to air flow stream.

$$\varepsilon = \frac{Q_{tower}}{Min(Q_{a,max}, Q_{w,max})} \tag{8}$$

Whillier correlated the effectiveness as a function of the capacity factor in terms of a single empirical constant. An alternative form that allows a more straightforward correlation of the data was employed by Lau (1983) and Hackner (1984) and is given as

$$\varepsilon = aR + b \tag{9}$$

where a and b are empirical constants that can be determined by linear regression applied to tower performance data. Generally, the value of b is close to 1 and a is between 0 and -1.

For given entering air and water conditions, the desired output of the model is the exiting water temperature. With the effectiveness evaluated from Equation 9, the exiting water temperature is determined directly from Equation 8 as

$$T_{cws} = T_{cwr} - \frac{\varepsilon\ Min(Q_{a,max}, Q_{w,max})}{m_{cw} C_{pw}} \tag{10}$$

The effect of cooling tower make-up water and the transient effects associated with the mass of the sump are neglected in this analysis.

The cooling tower fans are assumed to obey the fan laws. Given the power requirement at maximum fan speed, P_{max}, the power consumption of an individual fan is calculated as

$$P_{tower} = \gamma^3 P_{max} \tag{11}$$

where γ is the relative fan speed.

In order to test the accuracy of the Whillier model, coefficients of the tower effectiveness relation were fit to manufacturers' catalog data. Table 3 shows excellent agreement between predictions of tower heat rejection and the data for a range of conditions. Table 3 also compares results obtained with the more classical Merkel modeling approach. The accuracy of the two methods in modeling the performance of this particular tower are essentially the same. The root mean square of the error was 0.59 tons (2.07 kW) for the Whillier model and 0.96 (3.37) for the Merkel method. Similar results were obtained for other designs and conditions. The computational time required by the Merkel method is generally between 10 and 50 times that of the Whillier model, depending upon the conditions. There appears to be no advantage to the use of the Merkel model. The Whillier model requires neither numerical integration nor an iterative solution to determine exit states.

Results of the cooling tower model were fit to data for a three day period from the D/FW airport. D/FW measurements included the entering and leaving tower water temperatures. Ambient wet bulb temperatures were available from the National Weather Service for this time period. The maximum tower air flow rates and the coefficients of the effectiveness relation were unknowns in the regression analysis. As exhibited in Figure 1, the model is accurate to within about 2F (1C). Since the differences between the entering and leaving temperatures were in

the range of 5 to 15F (3C to 8C), large relative differences occur in the tower heat rejection rates.

Pumps

Three fixed-speed pumps, two 500 hp (373 kW) and one 250 hp (186 kW), are available for delivering water from the cooling tower sump to the chiller condenser. No direct measurement of condenser water flow rates was available. The overall pump and motor efficiencies were determined from manufacturers' data to be 0.76 at design conditions. Estimates of pump flow rates were made from measurements of pump supply pressures for different combinations of pumps operating and assuming full power input at the design efficiency. These are summarized in Table 4.

This study also considers the use of variable-speed condenser pumps. In order to estimate the power requirement associated with a particular flow for variable-speed operation, the following form was used for evaluating the system's pump head requirements.

$$H_s = a + b\dot{m}_{cw}^2 \tag{12}$$

The coefficients a and b were fit to D/FW supply pressure measurements. The power requirement for any particular flow is then

$$P_p = \frac{\dot{m}_{cw} g H_s}{\eta_p} \tag{13}$$

where η_p, the overall efficiency of the pump and motor, is again assumed to be 0.76 and g is the gravitational constant.

The primary chilled water pump is operated with a variable speed motor. Direct measurements of the chilled water flow are recorded by the data acquisition system. Throughout this study, measurements of the chilled water flows are utilized.

PERFORMANCE AND CONTROL CHARACTERISTICS OF THE D/FW PLANT

In this section, different aspects of the performance and control characteristics of the D/FW system are presented. The power consumption associated with the centrifugal chiller having variable-speed control is compared with that for constant-speed operation. The overall performance of the combination of the chiller, cooling tower and pumps is also investigated.

Variable-Speed versus Fixed-Speed Chiller Control

The part-load performance of a centrifugal chiller depends upon the method by which the capacity is modulated. The performance of the D/FW primary chiller operated with variable-speed control was compared with that associated with fixed-speed vane control. Tests were performed at the D/FW airport facility for both types of control at nearly identical conditions. Tables 1 and 2 summarize the results of these tests. The chilled and condenser water flow rates were held constant for these tests. The compressor speed for the vane control tests was held constant at 4000 rpm, and the inlet pre-rotation and outlet diffuser vanes were operated using the automatic control implemented by the manufacturer.

At all part-load conditions, the performance associated with the variable-speed control is superior. However, the power requirements come together at loads approaching the capacity of the chiller. This is to be expected, since at this condition the vanes are open wide and the speed under variable-speed control approaches that of the fixed-speed operation.

There is more inconsistency in the results of the fixed-speed tests (Table 2). For example, in comparing the results of tests 7 and 8 (or 13 and 14), the only condition that changed appreciably was the leaving condenser water temperature. However, the power

consumption associated with vane control did not increase as would be expected. In this mode of operation, both the inlet and outlet vanes are adjusted in some automatic fashion to meet the desired conditions. Therefore, it is possible to realize the same conditions with different power consumptions. The inconsistencies in the fixed-speed results may be due to less than optimal control of the inlet and outlet compressor vanes.

In order to see the differences between variable-speed and fixed-speed operation more clearly, the performance was correlated for both methods of control as outlined in the preceding section. Figures 2 and 3 show the chiller performance in terms of coefficient of performance (COP) as a function of load for different condenser to evaporator leaving water temperature differences.

Figure 4 shows a direct comparison of the results of Figures 2 and 3. The ratio of the power under variable-speed control to that with vane control is plotted as a function of load and leaving water temperature differences. The magnitude of the improvement of the variable versus the fixed-speed control is significant. At typical summer conditions of 5500 tons (19.3 MW) and temperature differences of between 40F and 50F (22C and 28C), the performance is quite similar. As the load decreases, the COP of the variable-speed control increases, while that associated with fixed speed operation is reduced. At part-load conditions of about 3000 tons (10.5 MW) and temperature differences between 30F and 40F (17C and 22C), the variable-speed control uses about 30% less power.

Figures 5 and 6 present simulated comparisons of the power consumption of the chiller for the two control strategies for periods of high and moderate chilled water loads. For the three days in June (Figure 6), the differences in chiller power consumption are relatively small (1.5% overall). For the October period, however, the total power consumption of the variable-speed and fixed-speed control chiller are 111 MWh and 157 MWh, respectively. The overall improvement through the use of the variable-speed operation is about 40%.

System Performance

The power consumption of the chiller is sensitive to the condensing water temperature, which is, in turn, affected by both the condenser water and tower air flow rates. Increasing either of these flows reduces the chiller power requirement but at the expense of an increase in the pump or fan power consumption. At any given load, chilled water setpoint, and wet bulb temperature, there exists an optimum operating point.

Figure 7 shows the simulated power consumption of the chiller, condenser pumps, and tower fans plotted versus the relative tower air flow rate for different numbers of tower cells operating at a relatively lightly loaded condition. The relative tower air flow is the ratio of the sum total of the all tower air flows to the maximum total flow for all cells operating at maximum speed. All cell fans were assumed to be operated at the same speed and a single 250 hp (186 KW) pump was employed.

When variable-speed fans are employed with the cooling tower, Figure 7 shows that the best strategy is to operate as many cells as possible, each at reduced air flows. For a given set of inlet conditions, the Whillier and Merkel models both indicate that the tower performance depends primarily upon the ratio of mass flow rates of the air and water streams. Thus, for given total air and water flow rates, the thermal performance associated with the tower is practically independent of the number of cells, since the flow rate ratio is constant. However, the power consumption of the tower fans depends upon the cube of air flow. Thus for constant total flow, it is best to operate as many fans in parallel as possible at reduced air flows. The optimal air flow for four-cell operation is about 40% of the maximum possible at the conditions of Figure 7.

The combined effect of both air and water flows on the power requirement of the chiller and variable-speed cooling tower fans and condenser pumps is presented in Figures 8-10. Contours of constant power consumption are plotted versus relative air and water flows for low, moderate, and high chiller loads. The relative air flow is as previously defined with four cells operating. The relative water flow is the ratio of the water flow rate to a maximum flow associated with the original two 500 hp (373 KW) pumps operating simultaneously. The operating point associated with the minimum total power consumption is shown with a single symbol. Each contour line away from the minimum represents a power increase of 5%.

The most surprising result concerning these performance maps is the flatness of the optimum. Near the optimum, power consumption is relatively insensitive to both flow rates.

Away from the optimum, power becomes more sensitive to these variables.

The optimum operating point is very sensitive to the chiller loading. Both the optimum relative water and air flows change from about a third to a half to three quarters from the low to moderate to high loads of Figures 8-10. Results presented in this way are useful to plant operators in defining "near optimal" manual control.

The load on the chiller for the results of Figure 10 is essentially at the capacity of the machine for the particular drive utilized. The optimal air and water flows are much lower than the maximum possible values. The cooling towers and condenser pumps were originally sized for much higher loads than the current system requirements.

The contours shown in Figures 8-10 exhibit a change in shape that occurs through the line labeled "R=1." This line passes almost exactly through the optimal operating point in all cases. The operating conditions along this line are such that the thermal capacities of the air and water streams through the cooling tower cells (Equations 6 and 7) are equal. The heat transfer across the tower is the effectiveness times the minimum thermal capacity rate. For a highly effective cooling tower, such as the D/FW design, the effectiveness varies over a relatively small range (on the order of 10%). In this case, the tower heat transfer increases almost linearly with the minimum thermal capacity rate. On the other hand, increasing the maximum thermal capacity rate changes only the effectiveness of the cooling tower. Thus the tower heat transfer characteristic changes abruptly at a thermal capacity factor, R, of unity (Equation 5). If R is less than one, increasing the minimum thermal capacity has a much more dominant effect than increasing the maximum thermal capacity. For the D/FW design, this results in optimal operation at a capacity factor of 1.

The cooling towers and chiller condenser at the D/FW airport are oversized relative to current loads. In order to investigate whether operation at a tower capacity factor of one is a general rule of thumb, the system was simulated as it was originally designed. Results of the mechanistic chiller model described in Braun, et al. (1987) were used for a refrigerant charge of R-22 and chiller capacity of 8700 tons (30.6 MW). The optimal operating points and associated tower capacity factor were determined for a range of conditions. The effect of a lower tower effectiveness at a tower capacity factor of unity was also considered. These results are summarized in Table 5.

For the D/FW system, the optimal relative air and water flows correspond to a tower capacity factor of unity, even for the original design operating at high loads. However, if the cooling tower effectiveness were lower, higher air flow rates are optimal and the associated optimal capacity factor falls below one. It is interesting that the optimal relative air and water flows associated with the original design are near their upper limits at the original design load.

The fact that for a highly effective cooling tower, optimal operation occurs when thermal capacities of the air and water streams are equal is useful in the context of optimal control. In this case, Equations 6 and 7 provide a relationship between the air and water flow rates and only a single variable optimization is required.

The effect of optimal control of the condenser water and cooling tower air flows on the plant performance was investigated using an optimization technique applied to the simulation model. The power consumption associated with optimal control of the chiller, tower fans, and condenser water flow was compared with that associated with the D/FW control for three-day periods in October and June. It was assumed that the existing condenser pumps were replaced with variable-speed equipment having the same maximum flows and power requirements. Table 6 summarizes comparisons between the optimal power requirements and those that result from the D/FW control. The reductions in total power consumptions with the use of optimal control of condenser water and cooling tower air flow rates for October and June periods are approximately 10% and 5%, respectively.

METHODOLOGIES FOR ON-LINE OPTIMAL CONTROL

In order to apply optimization techniques to determine optimal on-line control strategies, it is advantageous to have simple models of the cooling system that can be implemented on microcomputers. Parameters of these models could be continually updated with on-line system identification algorithms. If chilled water storage is employed within the system, it is

necessary to be able to forecast the cooling requirements several hours ahead. In this section, each of these topics is considered.

A Simplified System Model for Optimal Control

In the previous section, the power consumption of the cooling plant was determined using separate models of the individual components and by iteratively solving the set of simultaneous equations. The system simulation model was used along with a nonlinear optimization routine to determine optimal control. Although this model may be simple enough to be used in conjunction with optimal control, it is advantageous to further simplify the modeling process.

It was shown earlier that a quadratic relationship in two variables is adequate for representing the power consumption of the chiller. In considering the total power consumption of the chiller, cooling tower, and condenser water pumps, there are five important variables: (1) chilled water load, (2) chilled water setpoint, (3) ambient wet bulb, (4) condenser water flow rate, (5) tower air flow rate. If the tower cells operate with different air flow rates and/or there are multiple condenser pumps operating at different flows, then these are additional variables. Analogous to the bi-quadratic relationship for the chiller, the power consumption of the chiller, tower, and condenser pump subsystem can be empirically correlated using the following matrix quadratic relationship:

$$P = u'Au + b'u + f'Cf + d'f + f'Eu + g \qquad (14)$$

where

u = a vector containing the control variables: tower air and condenser water flow rates

f = a vector of forcing functions: chilled water load, chilled water setpoint and ambient wet bulb temperature

The matrices A and B, vectors b, d, and e, and the scalar g constitute empirical constants that must be fit to data. Since the equation is linear in the empirical coefficients, linear regression can be used. Although the chilled water setpoint is a control variable in the overall system, it is treated as a forcing function for optimal control of the condenser water loop.

The empirical system model given by Equation 14 was fit to simulated system performance data such as that used to generate Figures 8-10. Over a wide range of conditions, this model fits the data with a root-mean-square error of about 50 kW for power consumptions in the range of 1000 kW to 5000 kW.

Measurements at the D/FW facility include the chiller power consumption and the relative fan speeds of the tower cell fans. There are no direct measurements of the power requirements of the condenser pumps or cooling tower fans. It is possible, however, to estimate these power consumptions from the available measurements. Figure 11 shows results of a fit to total power consumption for three days of data in October. These results are very encouraging as to the applicability of Equation 14.

It is possible to use Equation 14 to directly determine the condenser pump and tower fan control that are optimal for any set of conditions. For unconstrained control, the minimum power occurs at a point where the partial derivatives of the power with respect to each control variable are zero. The optimal control is determined by the differentiating the matrix of Equation 14 with respect to the control vector, u, setting the result equal to zero and solving for u.

$$\frac{dP}{du} = 2u'A + b' + f'E = 0 \qquad (15)$$

Solving for the control vector gives

$$u = -0.5A^{-1}(b + Ef) \tag{16}$$

If the control determined by Equation 16 violates any constraints (i.e., maximum air or water flows), then it is necessary to apply the method of undetermined Lagrange multipliers to determine the constrained minimum.

Table 7 compares the optimal control points and associated power requirements from Figures 8-10 with those determined from Equation (16). Although there are significant differences between optimal relative water and air flow rates, the power consumptions as determined from the more detailed model at the control points determined with Equation 16, are within 50 kW. This good agreement is a result of the very flat optimums exhibited in Figures 8-10.

Time Series Models for Load Forecasting

Forecasting the cooling requirements of large building complexes is useful in minimizing energy consumption of cooling equipment when thermal storage is available. The cooling load is a function of many variables, such as ambient temperature, solar radiation, occupancy of people, lighting, electrical usage, etc. All of these heat gains are periodic functions having a dominant period of 24 hours. There are also random components in the loads resulting from the stochastic nature of the weather and the way in which the buildings and the distribution system are utilized. Therefore, a combined deterministic plus stochastic model is appropriate for load forecasting.

For on-line optimal control of the equipment, it would be advantageous to utilize on-line recursive parameter estimation for the forecasting model. Recursive parameter estimation is most easily carried out with linear models (i.e., the model is linear in the unknown parameters). For that reason, this study was restricted to linear time-series models termed AR (auto-regressive) models. A good background to material presented here is found in Pandit (1983).

An auto-regressive model of order n (AR(n)) has the form

$$X_t = \sum_{i=1}^{n} \phi_i X_{t-i} + e_t \tag{17}$$

where X_t is the current (zero mean) output of the system, X_{t-i} is the output i steps previous, ϕ_i is i^{th} parameter of the model, and e_t can be thought of either as a random input to the system or the one-step ahead prediction error of the model. In order to estimate parameters of the model for a given set of data, the sum of the squares of the prediction errors (e_t's) is minimized with respect to the unknowns ϕ's.

Simple AR models given by Equation 17 were fit with March cooling load data for a sampling interval of one hour. An AR(4) model giving a root-mean square (rms) error of 329 tons (1.16 MW) for a one-step prediction was found to be statistically adequate for this data. Comparisons of the one-step and five-step ahead predictions with the data are shown in Figures 12 and 13. The AR(4) model does reasonably well for the one-hour prediction but falters badly with five hour forecasts.

An improved model results if some of the determinism is removed by fitting a trigonometric polynomial to the data. The periodic trends in the data can be removed by the use of a trigonometric polynomial of order m, having the form

$$P(t) = \sum_{j=1}^{m} a_j \sin(j\omega t) + \sum_{j=1}^{m} b_j \cos(j\omega t) \tag{18}$$

where ω is the frequency and the a's and b's are unknown coefficients that are fit with a linear least squares method applied to the data.

A combined model can also be expressed in a linear form. The combined model for a zero mean output, Y_t, is the sum of the deterministic and stochastic models.

$$Y_t = \sum_{j=1}^{m} a_j \sin(j\omega t) + \sum_{j=1}^{m} b_j \cos(j\omega t) + \sum_{i=1}^{n} \phi_i X_{t-i} + e_t \tag{19}$$

But, by definition,

$$X_t = Y_t - \sum_{j=1}^{m} a_j \sin(j\omega t) + \sum_{j=1}^{m} b_j \cos(j\omega t) \tag{20}$$

Substituting Equation 20 into 19 gives

$$Y_t = \sum_{j=1}^{m} c_j \sin(j\omega t) + \sum_{j=1}^{m} d_j \cos(j\omega t) + \sum_{i=1}^{n} \phi_i Y_{t-i} + e_t \tag{21}$$

where the c's and b's are different coefficients than those appearing in Equation 19.

All the coefficients of Equation 21 can be fit to data with linear least-squares methods. For batch computations, the data are averaged and the average is subtracted from the data before the fitting process.

If a combined model is fit to the data, then the adequate model again has four autoregressive parameters and two periods (i.e., n=4, m=2). In this case, the rms error is 287 tons (1.01 MW). This is a significantly improved model over the pure AR(4) (rms of 329 ton [1.16 MW]). Figure 14 shows a comparison between the five-step ahead predictions of the combined model with the March data. In addition to the improved one-step predictions, the ability of the model to perform five hour ahead forecasts is vastly improved. The rms of the errors for five step predictions of the combined model is 398 (1.40), as compared with 625 (2.20) for the pure AR(4).

Even better five hour predictions can be realized by using a larger sampling interval for the data. The model determined with a 2.5 hour sampling interval gives significantly better results for the long-term predictions (rms of 296 [1.04] versus 398 [1.40]. The larger sampling period more appropriately captures the larger scale variations in the data. The forecasts associated with a five hour sampling interval are better still.

A good test of the model determined with the March data is to compare it with another data set. A comparison with October data gave good results for a one-step prediction, but the five-step forecast was very poor. There is a seasonal effect that alters the characteristics of the deterministic part of the data. The cooling requirement is coupled closely to the ambient temperature. Generally, the peak cooling load occurs at about the same time of the day as the maximum ambient temperature. During October this peak occurs later in the day than in March.

The linear model given by Equation 21 may be fit using on-line recursive parameter estimation as outlined by Ljung (1983). Given initial guesses of the parameters, updated values are determined at each step according to the relation

$$\psi[t] = \psi[t-1] + L[t]e_t \tag{22}$$

where $\psi[t-1]$ is a vector of current estimates of the parameters, $\psi[t]$ are the updated estimates, and $L[t]$ is a gain matrix that minimizes the sum of squares of the errors over all time up to t (see Ljung 1983). Since the mean of the data is not known a priori with this on-line identification scheme, it is necessary to include it as an unknown parameter in the

model. In this study, all data points were equally weighted. It is possible with on-line identification to use higher weighting for more recent data.

The advantage of recursive on-line identification for this process is that changes that occur in the model on a seasonal basis, such as those discussed for the October and March data, will allow adjustments to be made in the model. This can be accomplished in two ways. First, the incoming measured data may be weighted more heavily than past data (e.g., exponential weighting) so that the parameter estimates more correctly reflect the current state of the system. This was not necessary for this analysis, since the data set was limited. Secondly, periodicities that reflect seasonal changes in the climate or building occupancy may be included.

On-line recursive parameter estimation was applied to a set of data that utilized the March data twice in sequence. This procedure was chosen in order to allow the model sufficient time to track the data. Figure 15 shows comparisons between one-step-ahead predictions of the recursively identified model and the data at each step of the recursive procedure. The initial prediction at the start is 0, since the initial parameters were taken to be zero. A relatively short period of time is required in order for the model to perform adequate one-hour forecasts. More continuous data are needed to test whether the model performs adequately under all conditions. Nonetheless, the results thus far are encouraging.

In an attempt to further improve the long-term forecasts of the model, the ambient temperature was used as a deterministic input to the model. At the D/FW airport, the cooling requirement is strongly coupled to the ambient conditions. However, since the ambient temperature and cooling requirement are essentially in phase, there was little improvement in the results with the additional information. In other words, the history of the ambient temperature is almost completely reflected in the cooling load history.

CONCLUSIONS

Simple models were presented for the chiller and cooling tower. The empirical chiller model fits data for both variable-speed control and fixed speed with vane control. The cooling tower model utilized in this study was developed by Whillier. Results of this model were compared with manufacturers' data, measurements from the D/FW airport, and with the more classical Merkel method. There appears to be no advantage to the use of the Merkel model. The Whillier model requires far less computational effort than the Merkol method with nearly identical results.

The performance of the D/FW chiller operated with both variable speed, (having wide open vanes) and fixed speed (with vane control) was compared for two different time periods. The variable-speed control provides only a 1.5% reduction in the power requirements for a summer period but a 40% reduction for fall conditions. The savings associated with the use of variable-speed control are very significant at part-load conditions.

The performance characteristics of the combination of the chiller, cooling tower cells, and condenser pumps were studied. When variable-speed fans are employed for the cooling tower, it is desirable to operate as many cells as possible. If variable-speed condenser pumps are utilized, then the optimal operating point for the D/FW system occurs at flows such that the thermal capacities of the air and water streams are equal. This result may prove to be useful in applying optimal control to the condenser water loop. Optimal control of the D/FW system resulted in a 5% reduction in the overall power requirements for a summer period and a 10% reduction for conditions in fall.

A simple empirical model for the chiller, cooling tower, and condenser pumps as a whole was developed. This model can be used to evaluate the optimal condenser water and tower air flow rates in a straightforward manner. Results of optimal control points determined with this method compared well with a more detailed analysis. It may be possible to apply a similar approach to the chilled water distribution and air-handling units in order to include the chilled water flow, chilled water setpoint, and supply air flows as control variables in the optimization.

Pure time series and combined deterministic plus time series models were fit to cooling load data for the D/FW airport using both batch and on-line recursive methods. In all cases, the models worked well for making one-hour-ahead forecasts. In order to make longer term

predictions, it was necessary to include deterministic components in the model. The resulting model is simple enough to be fit with linear least-square methods. The procedure for on-line recursive parameter estimation begins to track quite quickly, even when given poor initial estimates of the parameters. Load forecasting is necessary for on-line optimal control of a cooling plant that utilizes thermal storage. Further work is necessary to identify practical optimal control algorithms for plants with storage.

REFERENCES

ASHRAE. 1983. ASHRAE handbook equipment, Atlanta.

Braun, J.E., Mitchell, J.W., Klein, S.A., and Beckman, W.A. 1987. "Models for variable speed centrifugal chillers." ASHRAE Transactions, vol. 93, part 1.

Hackner, R.J. 1984. "HVAC system dynamics and energy use in existing buildings," M.S. Thesis, Mechanical Engineering, University of Wisconsin-Madison.

Johnson, G. 1985. Personal communication, York International.

Lau, A.S. 1983. "Development of computer control routines for a large chilled water plant," M.S. Thesis, Mechanical Engineering, University of Wisconsin-Madison.

Ljung, L., and Soderstrom, T. 1983. Theory and practice of recursive identification, Cambridge MA: MIT Press.

Pandit, S.M. and Wu, S.M. 1983. Time series and system analysis with applications, New York: John Wiley.

Whillier, A. 1967. "A fresh look at the calculation of performance of cooling towers," ASHRAE Transactions, vol. 82, part 1, p. 269.

TABLE 1
Empirical Fit to Variable-Speed Data

Test	Load (tons)	Leaving Evap. Temp. (F)	Leaving Cond. Temp. (F)	Power (kW) Measured	Model
1	1375	40	57	364	334
2	2475	41	64	650	688
3	2800	40	69	1010	1046
4	2750	40	79	1411	1505
5	2710	40	64	805	789
6	1355	50	57	126	156
7	5420	40	69	2416	2369
8	5460	40	76	2736	2835
9	5420	40	86	3580	3521
10	2690	50	62	415	405
11	2750	50	69	610	622
12	2730	50	82	1299	1338
13	4065	50	64	940	913
14	4065	50	75	1316	1358

TABLE 2
Empirical Fit to Fixed-Speed Vane Control Data

Test	Load (tons)	Leaving Evap. Temp. (F)	Leaving Cond. Temp. (F)	Power (kW) Measured	Model
1	1355	40	58	860	708
2	2625	40	62	1410	1480
3	2710	40	69	1800	1620
4	2670	40	80	1930	2084
5	2710	40	64	1410	1540
6	1625	49	57	1036	1065
7	5420	40	70	2780	2818
8	5420	40	76	2736	2974
9	5420	40	86	3627	3480
10	2710	50	62	1560	1635
11	2750	50	69	1326	1550
12	2730	50	82	1830	1734
13	4065	50	64	2446	2323
14	4065	50	75	2480	2220

TABLE 3
Cooling Tower Comparisons

T_{wb}(F)	T_{cwr}(F)	Manufacturers' Data		Heat Rejection (tons) Whillier	Merkel
65		90	89	88.6	87.8
70		95	99	98.2	98.6
70		87	50	50.0	49.5
72		95	89	89.2	89.6
72		92	71	70.7	70.4
73		96	91	91.1	91.6
75		97	86	87.8	88.5
75		95	75	75.1	75.0
78		97	72	72.7	73.2
78		95	60	59.4	60.2
79		96	60	60.1	61.0
80		96	54	53.4	55.0

TABLE 4
Estimated Condenser Pump Flows

Pump Operation	Flow (gpm)	Power (kW)
250 hp	6600	188
500 hp	11400	375
250 + 500 hp	15700	563
500 + 500 hp	17800	750

TABLE 5
Optimal Operating Conditions for R-22 Chiller

Minimum Tower Effectiveness	Load (tons)	T_{wb}(F)	Optimal Conditions Relative Water Flow	Relative Air Flow	R
0.9	5500	75	0.75	0.65	1.00
0.9	8500	75	0.95	0.79	1.00
0.9	8500	85	1.09	0.78	1.00
0.6	5500	75	0.82	0.85	0.80
0.6	8500	75	1.04	1.03	0.80
0.6	8500	85	1.11	0.99	0.73

TABLE 6
Optimal versus D/FW Control

Time Period	Power MWH D/FW	Optimal
October	132.2	120.7
June	207.7	198.8

TABLE 7
Optimal Control Comparison

Load (tons)	Equation (16) Relative Water Flow	Relative Air Flow	Power (kW)	Figures 8-10 Relative Water Flow	Relative Air Flow	Power (kW)
2000	0.45	0.52	865	0.34	0.38	825
4000	0.69	0.64	2625	0.61	0.54	2600
5500	0.84	0.75	4235	0.75	0.64	4200

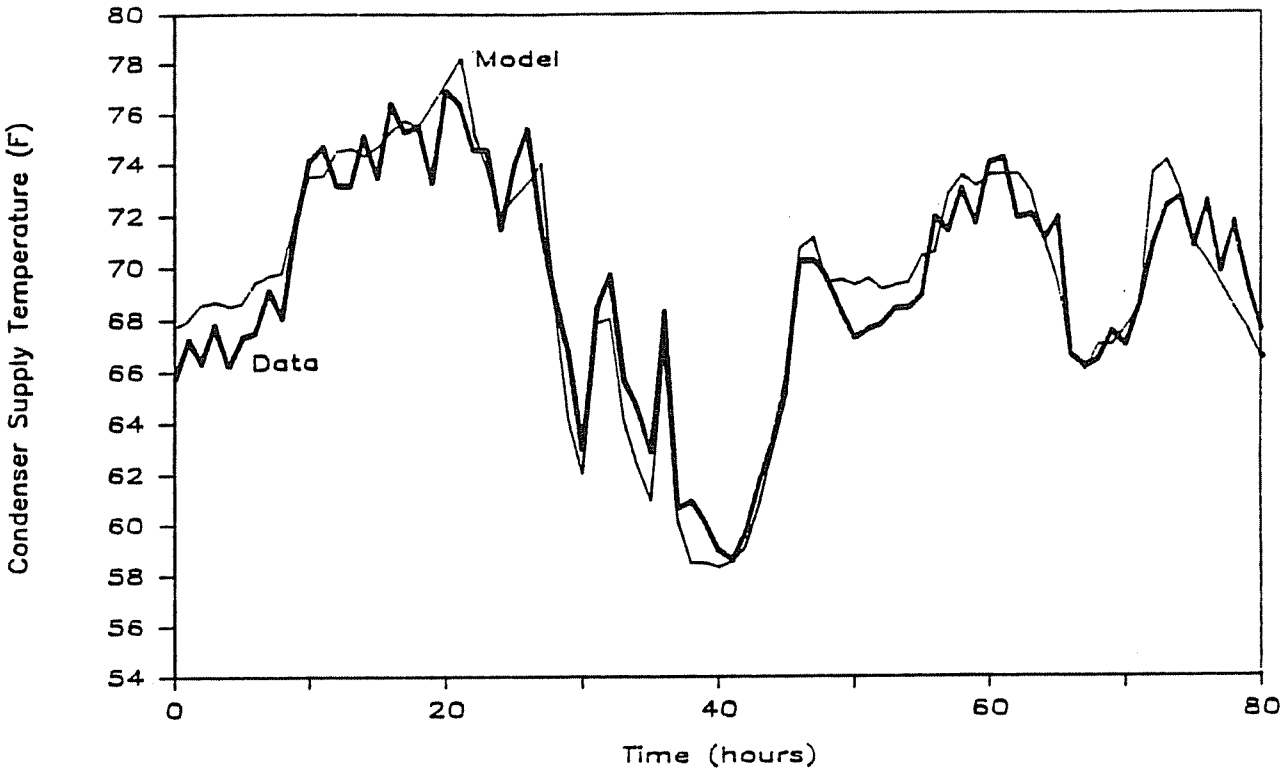

Figure 1. Comparisons between cooling tower and D/FW measurements

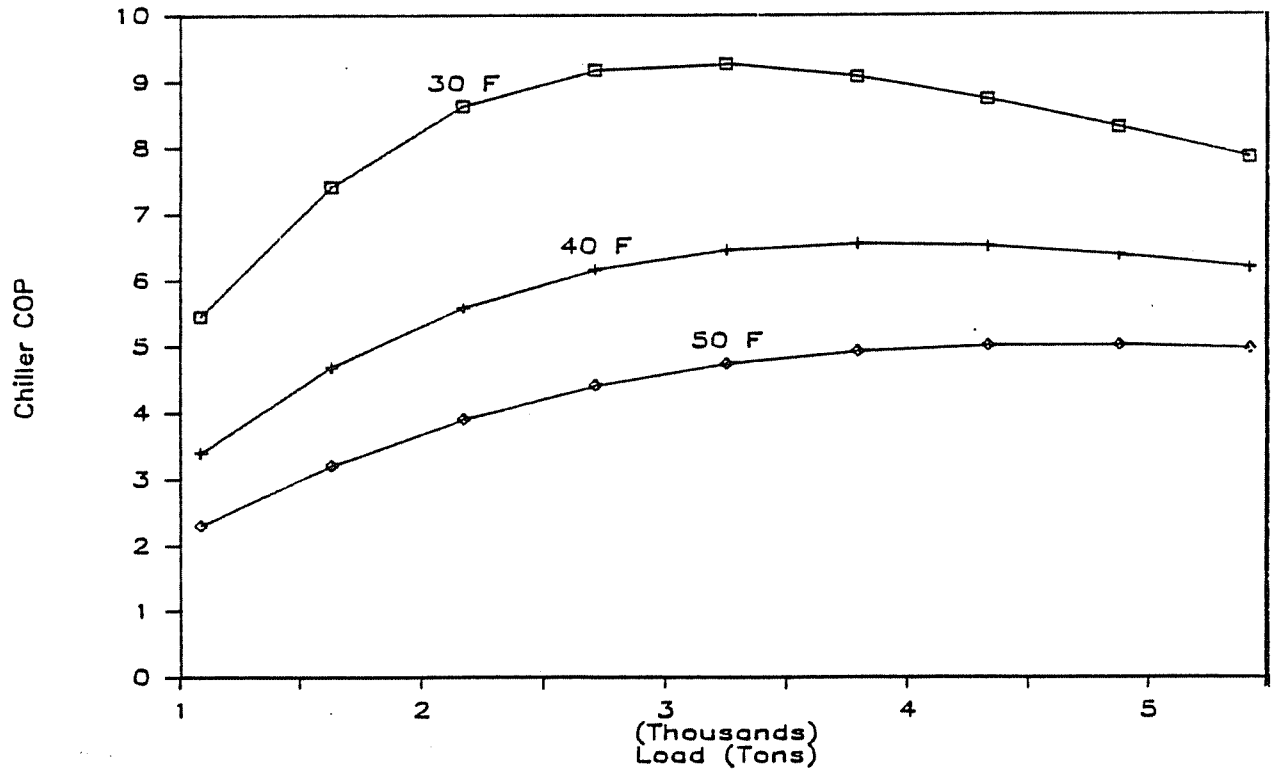

Figure 2. D/FW chiller performance for variable-speed control

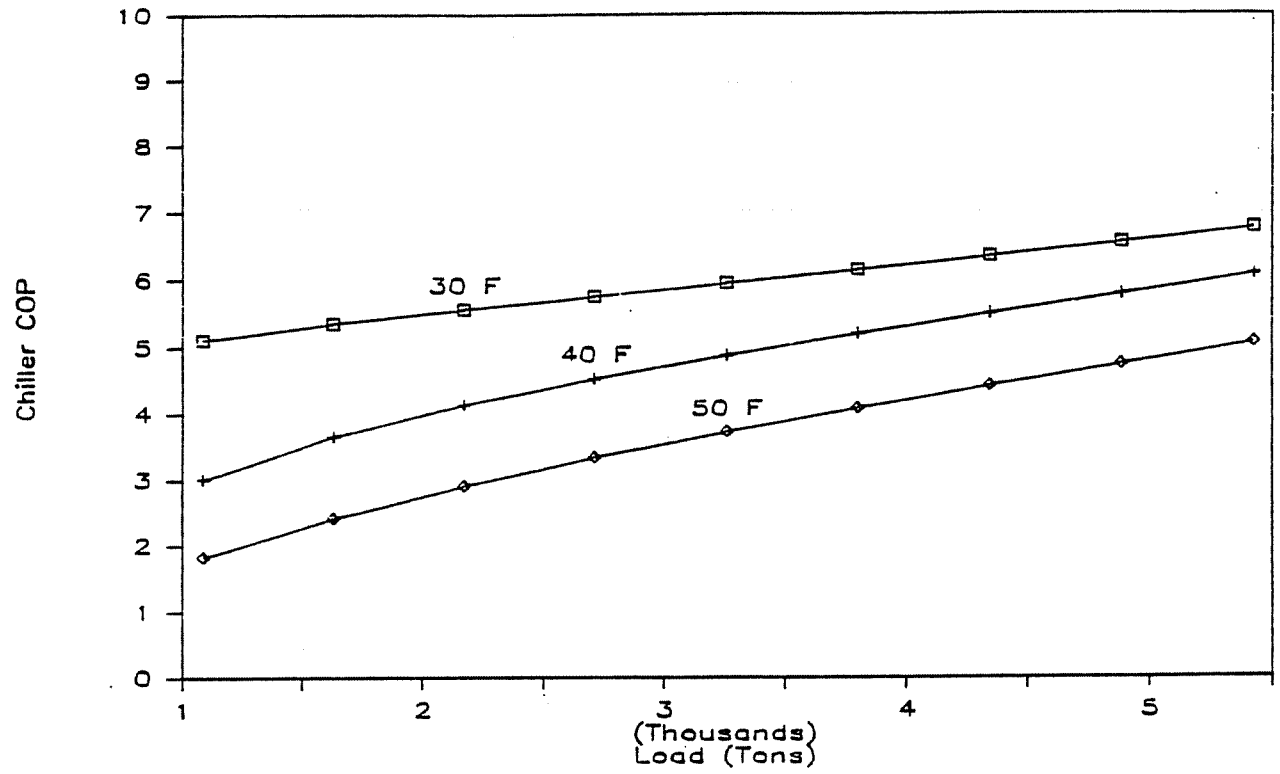

Figure 3. D/FW chillwer performance for fixed-speed, vane control

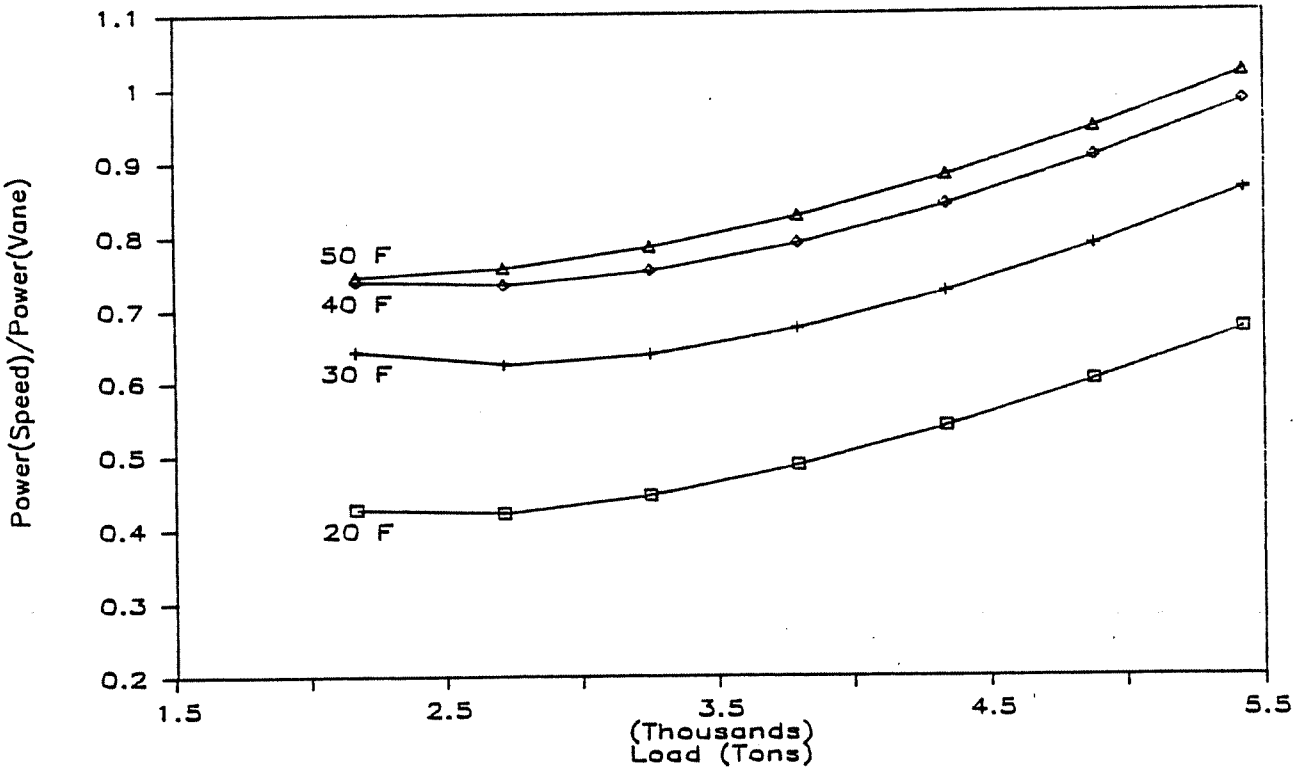

Figure 4. Comparison between the steady-state power requirements for speed and vane control

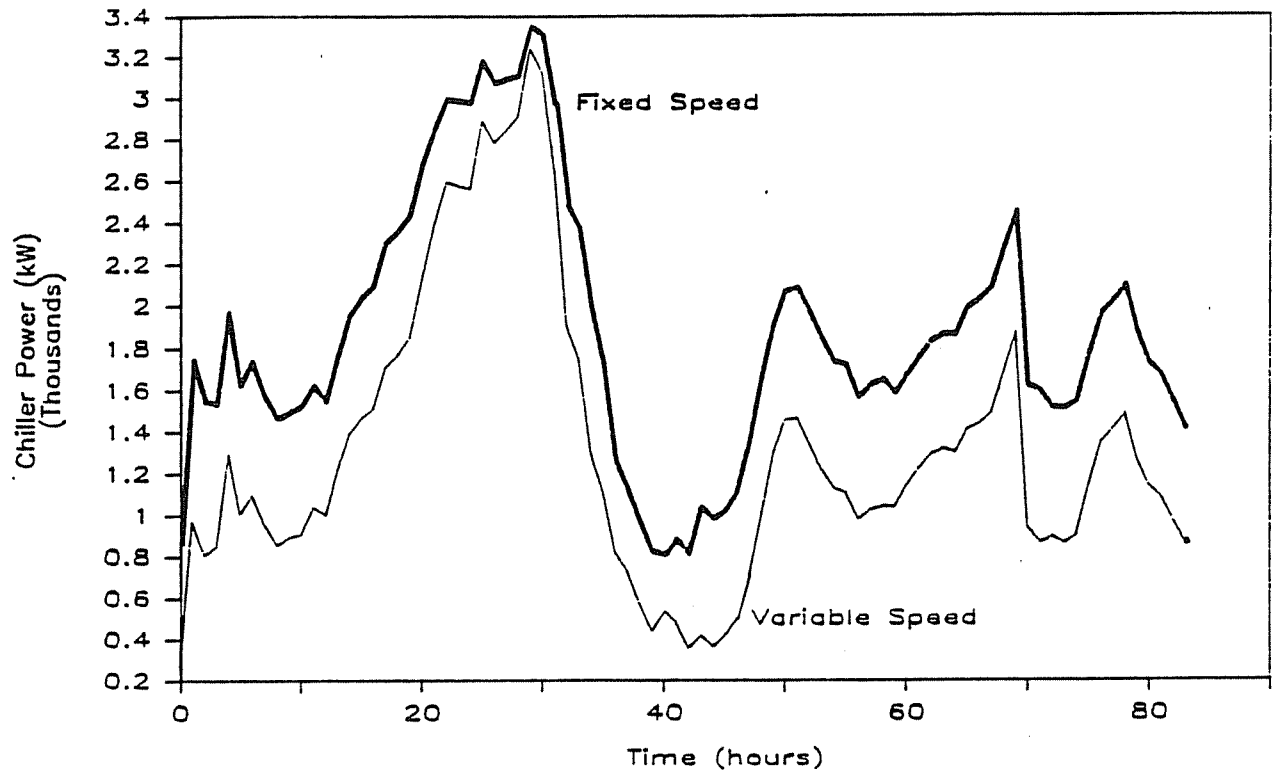

Figure 5. Comparison between the power requirements for speed and vane control during October

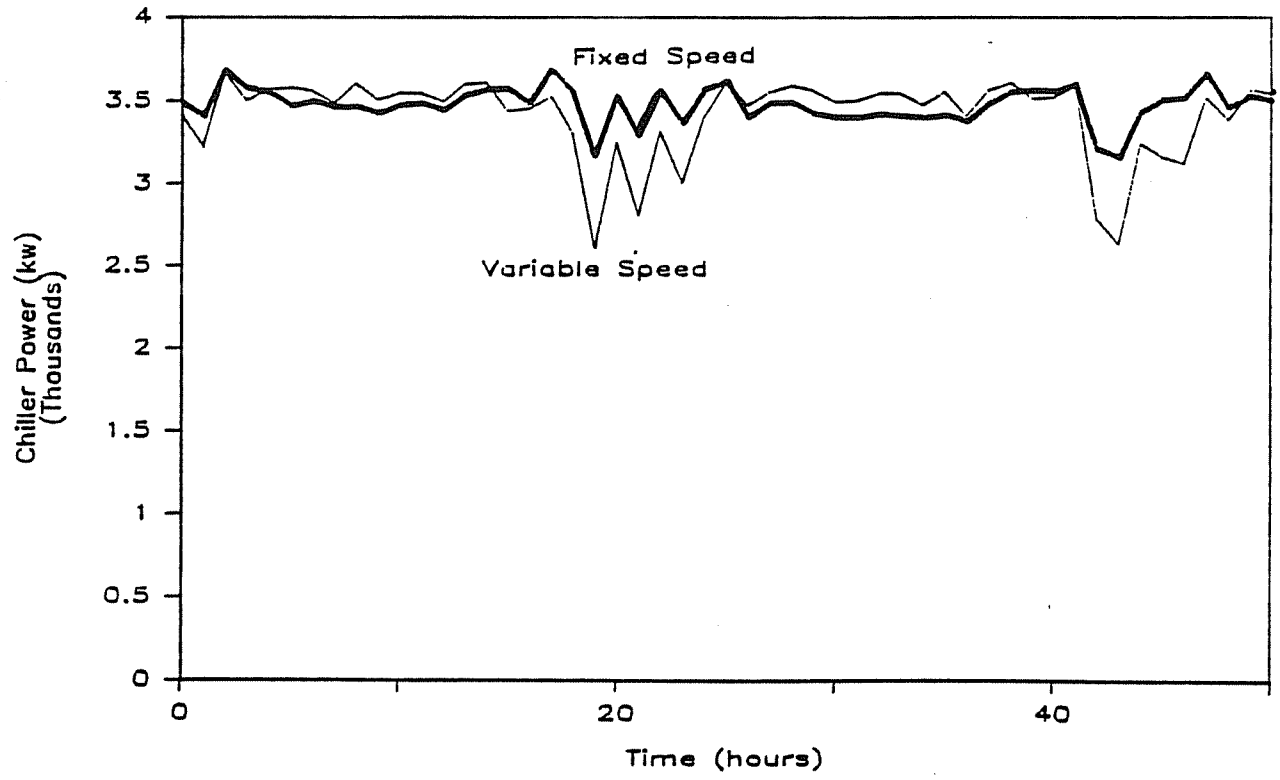

Figure 6. Comparison between the power requirements for speed and vane control during June

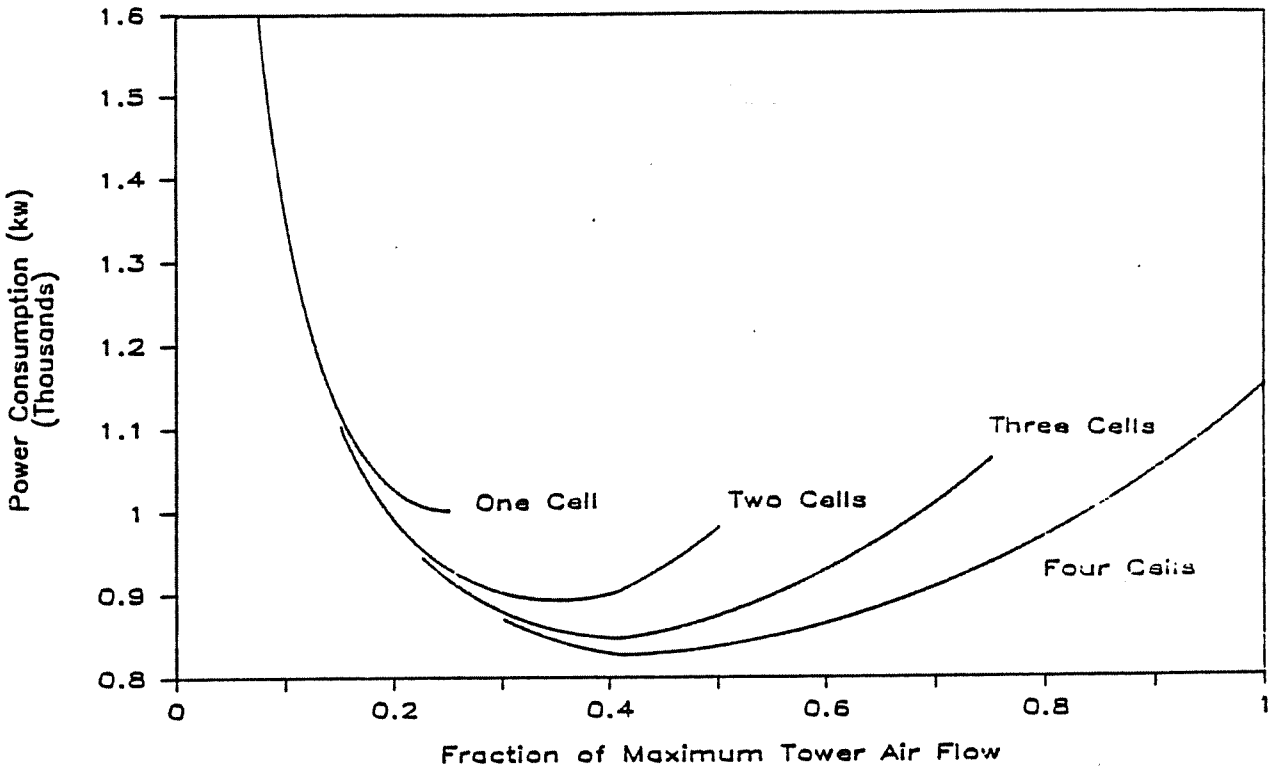

Figure 7. The effect of the number of cooling tower cells and airflow on the chiller and tower power consumption

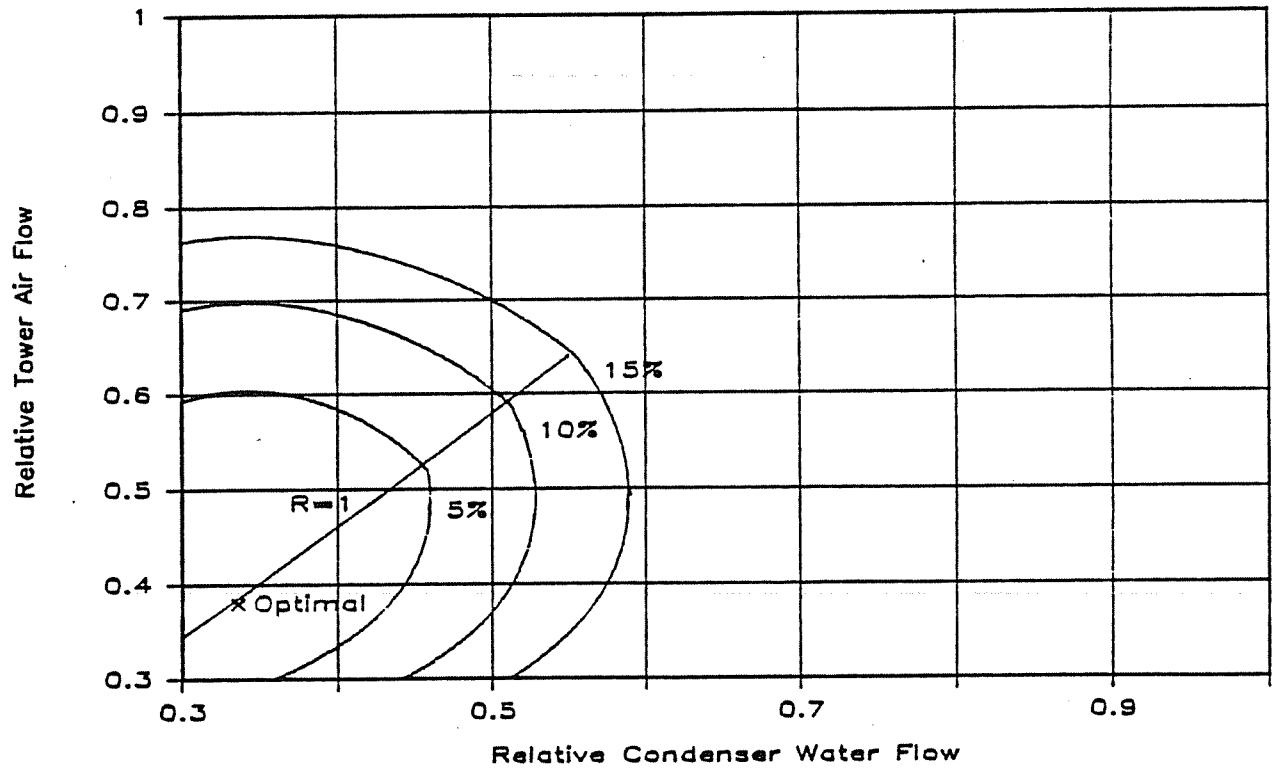

Figure 8. Power contours in terms of relative cooling tower water and airflows for a low load (2000 tons, chilled water setpoint of 50 F, ambient wet bulb of 65 F

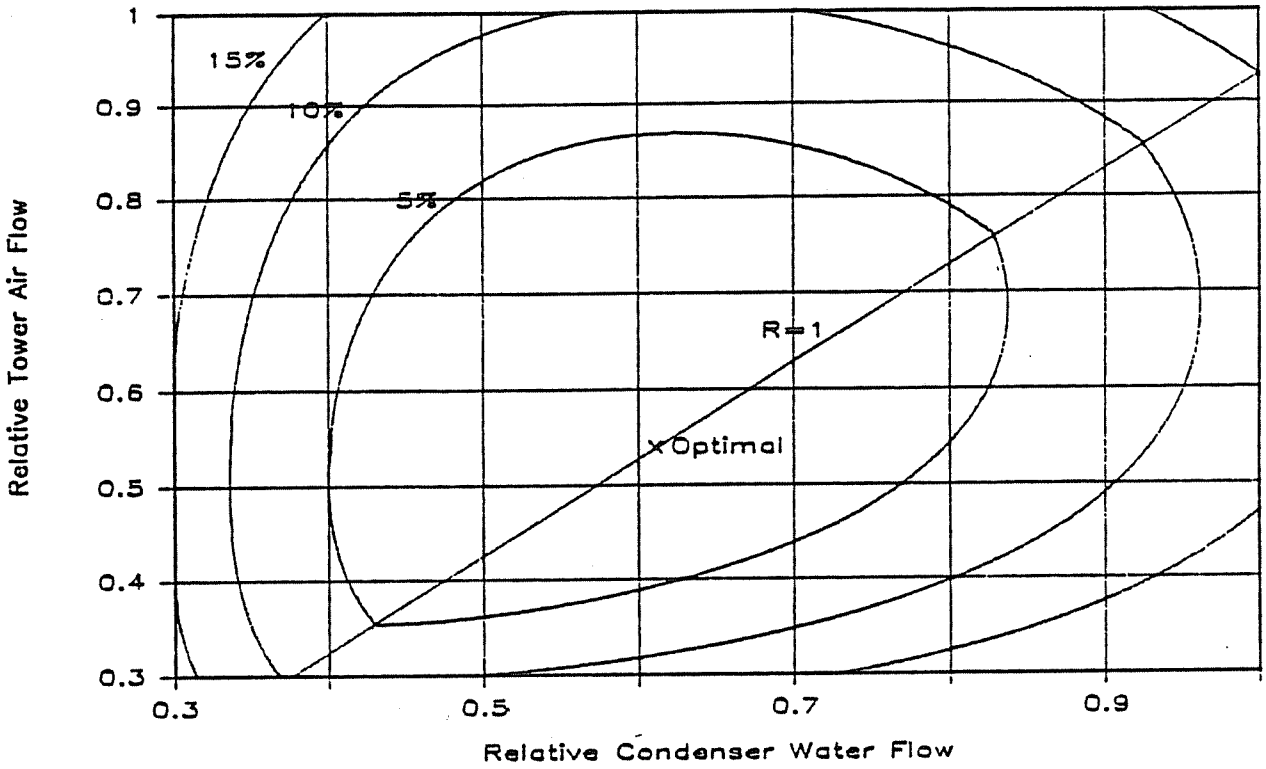

Figure 9. Power contours in terms of relative cooling tower water and airflows for a moderate load (4000 tons, chilled water setpoint of 45 F, ambient wet bulb of 75 F)

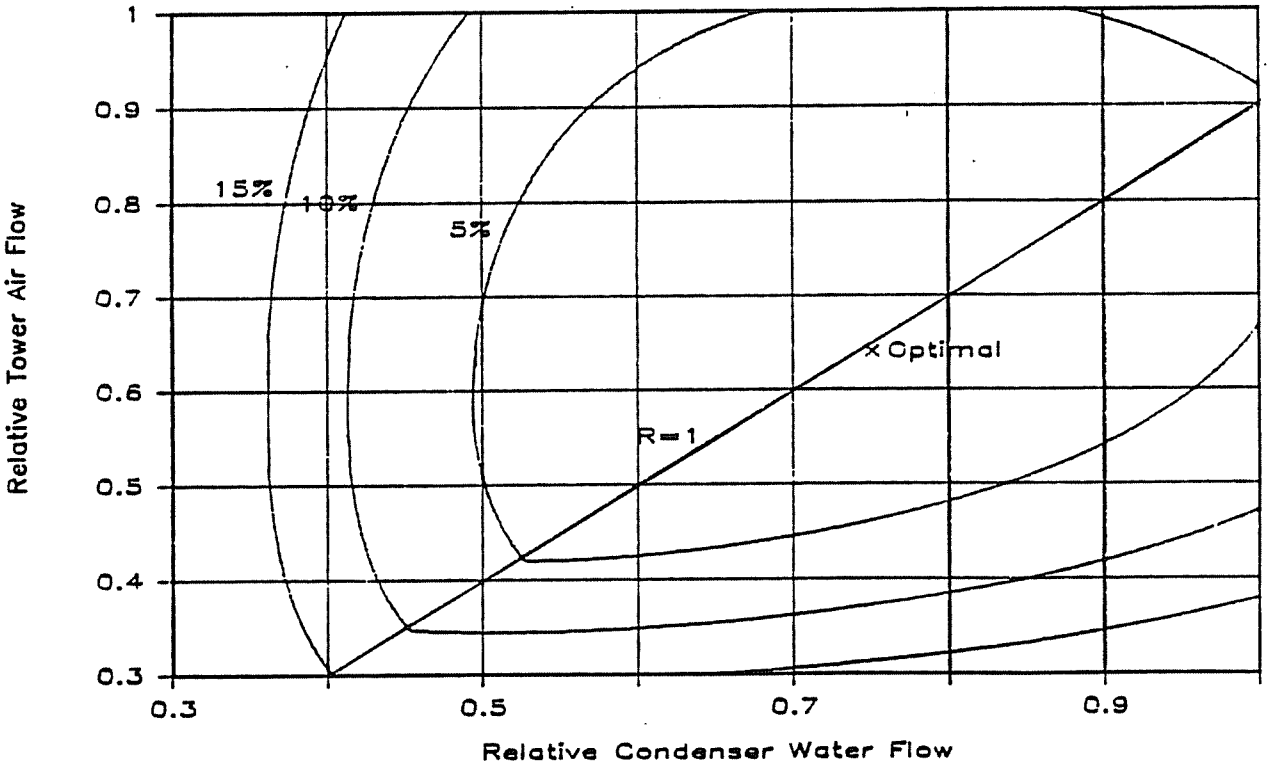

Figure 10. Power contours in terms of relative cooling tower water and airflows for a high load (5500 tons, chilled water setpoint of 40 F, ambient wet bulb of 75 F)

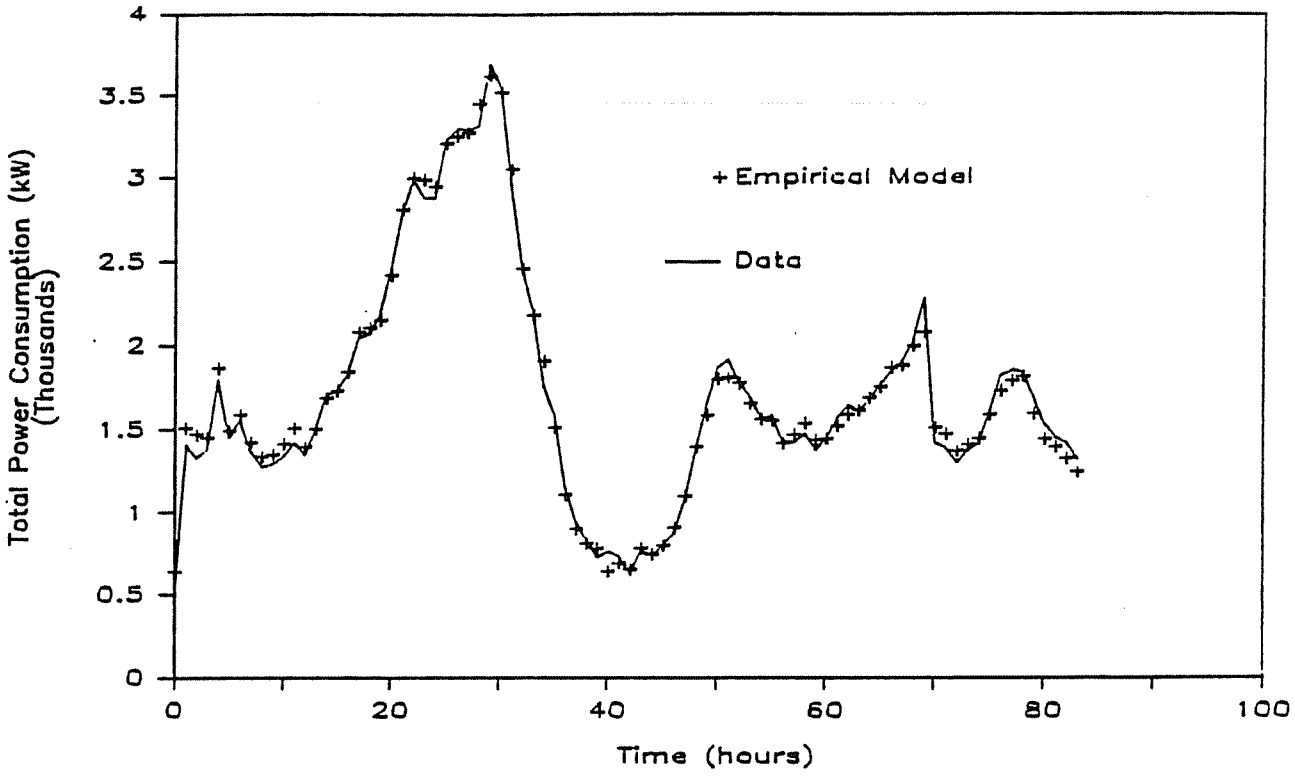

Figure 11. Comparison of empirical model of the chiller, cooling tower, and condenser pump power requirements with D/FW October data

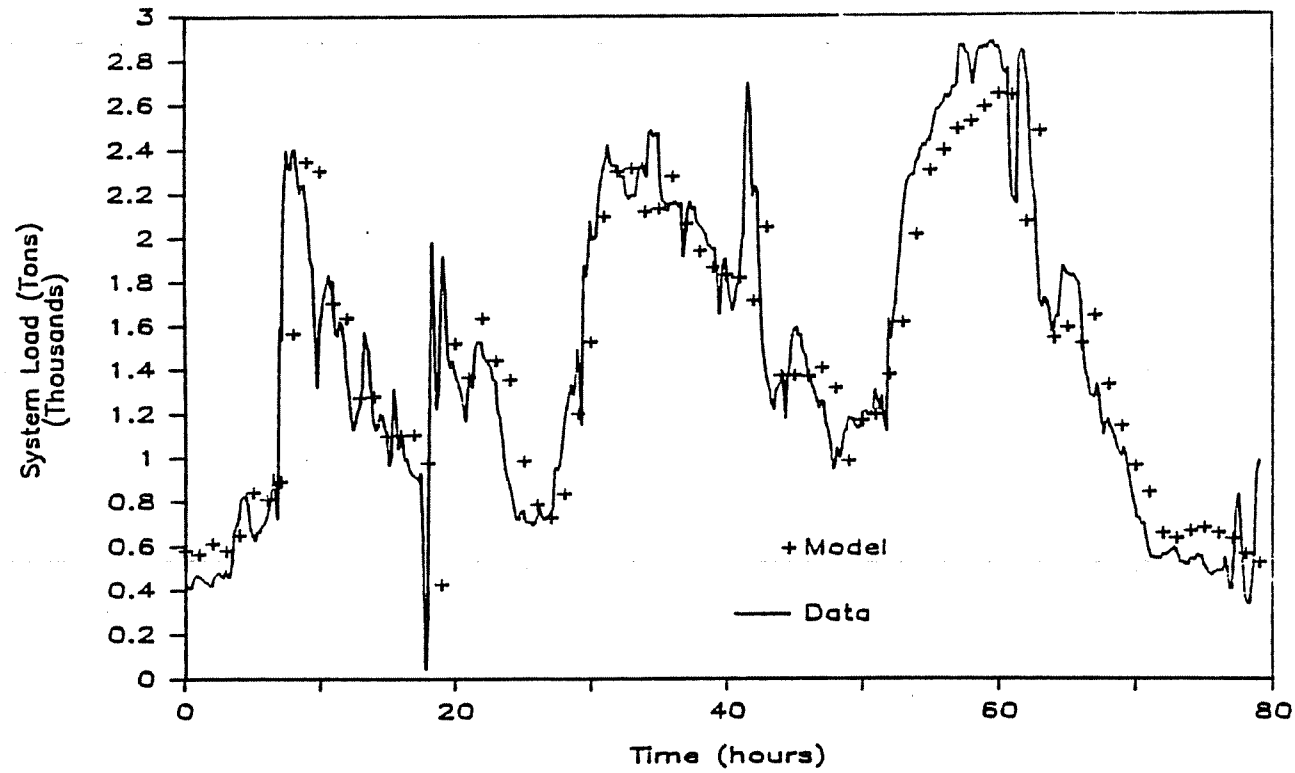

Figure 12. Comparison of AR(4) one-hour forecasts of cooling loads with March data

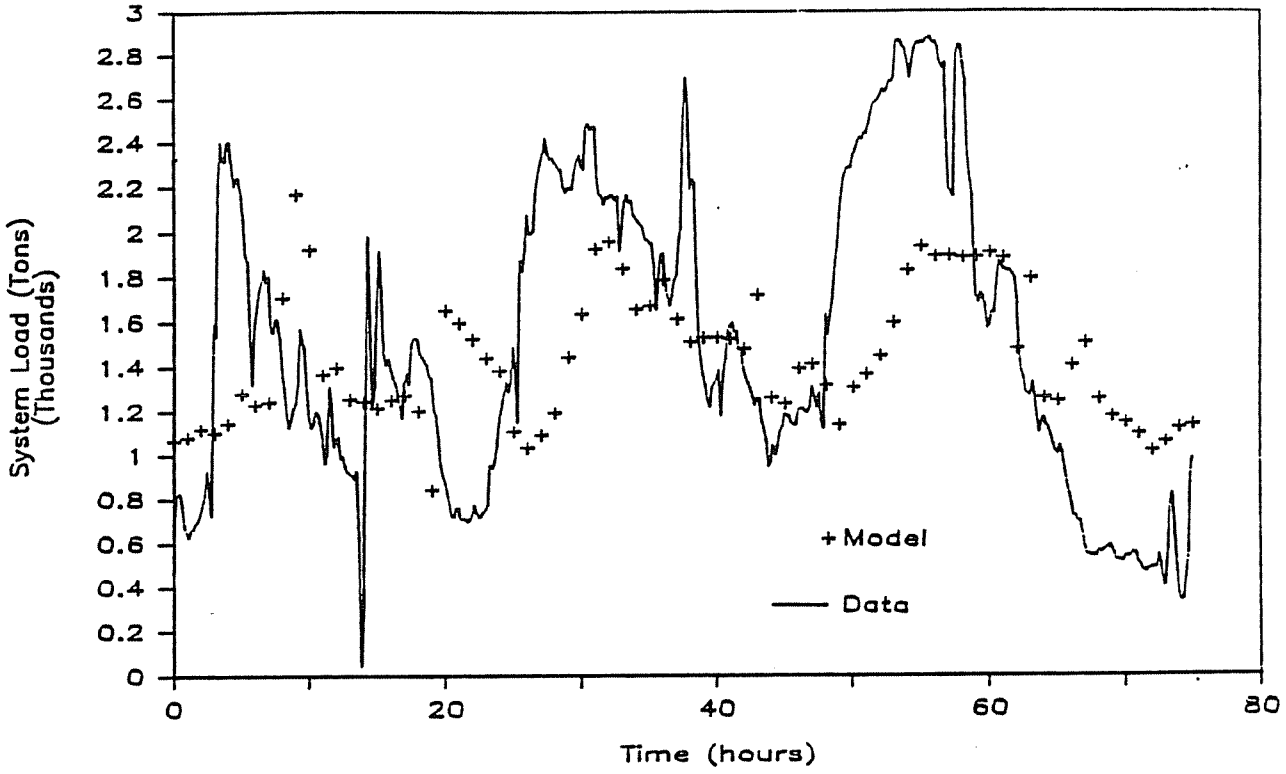

Figure 13. Comparison of AR(4) five-hour forecasts of cooling loads with March data

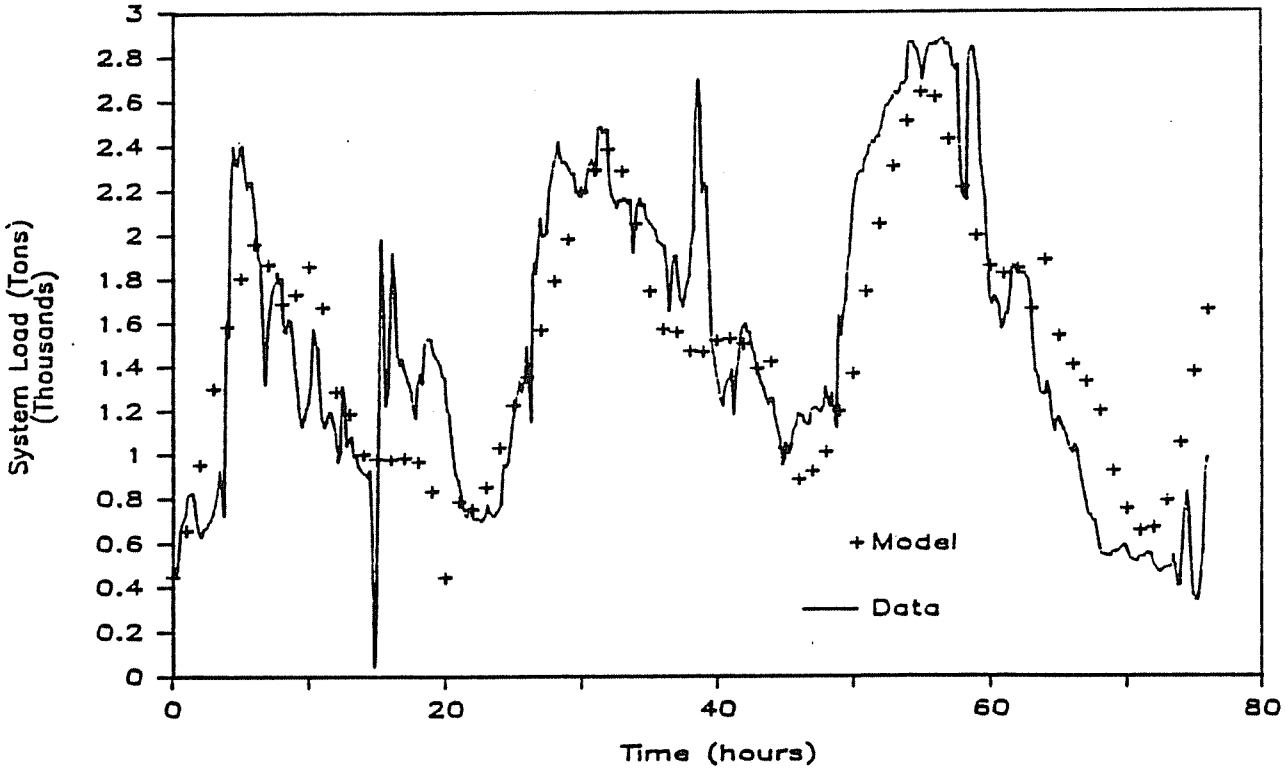

Figure 14. Comparison of combined model five-hour forecasts of cooling loads with March data

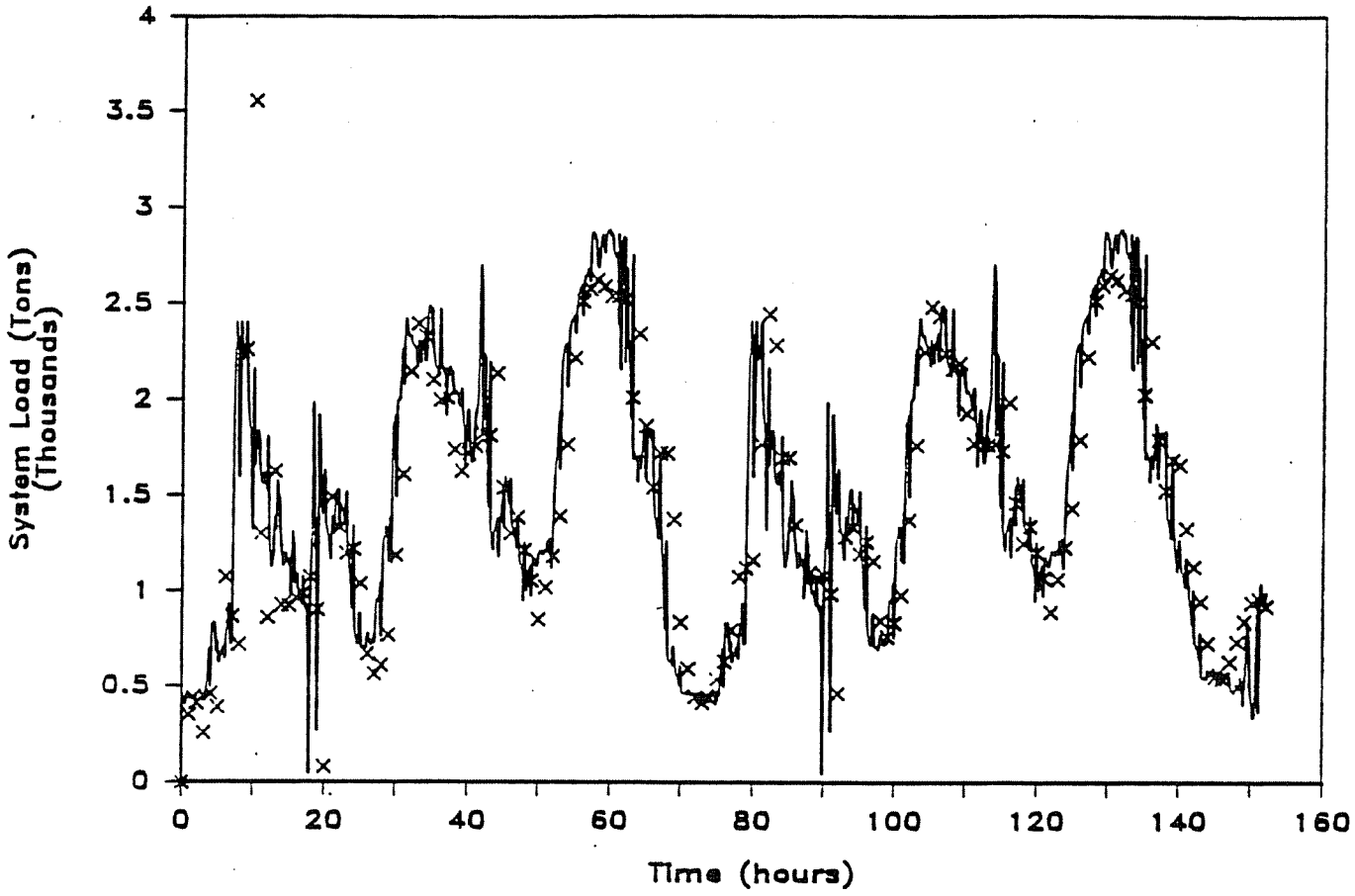

Figure 15. Recursive on-line parameter estimation of combined model applied to March cooling load